

See discussions, stats, and author profiles for this publication at: <https://www.researchgate.net/publication/225299833>

Dual Fluorescence of Graphene Oxide: A Time-Resolved Study

ARTICLE *in* THE JOURNAL OF PHYSICAL CHEMISTRY A · JUNE 2012

Impact Factor: 2.69 · DOI: 10.1021/jp301755b · Source: PubMed

CITATIONS

21

READS

49

3 AUTHORS, INCLUDING:



Xian-Fu Zhang

Institute of applied photochemistry, Hebei Pr...

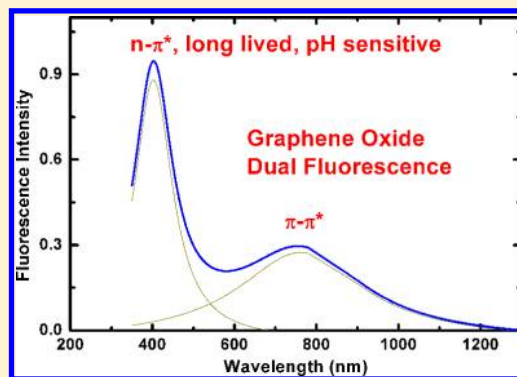
76 PUBLICATIONS 715 CITATIONS

SEE PROFILE

Dual Fluorescence of Graphene Oxide: A Time-Resolved Study

Xian-Fu Zhang,^{*,†,‡} Xiaona Shao,[†] and Suping Liu[†][†]Chemistry Department, Hebei Normal University of Science and Technology, Qinhuangdao, Hebei Province, China 066004[‡]MPC Technologies, Hamilton, ON, Canada L8S 3H4

ABSTRACT: The fluorescence properties of graphene oxide (GO) was studied by recording the fluorescence lifetime, fluorescence emission, and excitation spectra, as well as UV–visible and near-IR absorption spectra. For the first time, we showed that a blue band (ca. 440 nm) and a long wavelength (LW) band (ca. 700 nm) are coexistent, which can be recorded simultaneously by controlling concentration, excitation wavelength, and pH values. Two bands are closely related by the protonation or deprotonation of GO. The blue band is favored by low GO concentration, short excitation wavelength, and high pH value, while the LW band is favored by low pH and long excitation wavelength. To reveal the nature of the dual emission of GO, the fluorescence lifetimes under various conditions were also measured. The blue band contains three emitting components; one of them has a lifetime as long as 10 ns, and its emitting intensity is fairly sensitive to pH, showing the potential for applications in sensing H^+ and fluorescence lifetime imaging. Combining the results under various conditions, we conclude that the electronic transition for this component is very likely due to $n-\pi^*$ transition. The LW band contains two main emitting components (0.2 and 2.1 ns) that also appear in the blue band as minor contributors; the related emission is assigned to $\pi-\pi^*$ transition. In summary, GO emission is of broadband (300–1250 nm), long-lived, pH sensitive, and excitation wavelength dependent. This makes it easily tailored for versatile applications.



■ INTRODUCTION

Graphene materials are being heavily exploited for various applications,^{1–13} including biosensing^{3,14,15} and optoelectronic devices.^{4,16,17} A perfect single-layered graphene sheet, in which every carbon atom is sp^2 hybridized and π -conjugated with adjacent carbons, is a zero band gap semiconductor and not expected to be photoactive or photoluminescent. Graphene oxide (GO) and the corresponding chemically reduced GO (rGO) are actually chemically functionalized graphene that retain many properties of the highly valued pure graphene. Some carbon atoms of GO are bonded with oxygen atoms in the form of epoxy, hydroxyl, carbonyl, and carboxyl. The presence of the functional groups transforms some of sp^2 carbons to sp^3 ones, resulting in structural defects that give GO and rGO a finite band gap and forming many isolated sp^2 carbon clusters. Therefore GO and rGO are photoactive and photoluminescent. This causes remarkable light absorption, broadband emission, and hence rich optoelectronic properties for GO and rGO, in contrast to the perfect graphene material. As a result, GO and rGO have received significant attention for their potential uses in low-cost, large-area optoelectronic applications. The fluorescence of GO occurs in the UV, visible (vis), and near-infrared (NIR) wavelengths range, a property useful for biosensing, live cellular imaging, fluorescence tags, and nonlinear optical materials for ultra fast lasers.³

Regarding GO fluorescence, Sun and Dai reported green (peak maximum around 570 nm) and NIR emission in aqueous dispersion,⁵ which was later confirmed by other investiga-

tions.^{18–22} Cuong et al. recorded a fluorescence maximum at ca. 600 nm for GO film. Chen and Yan reported emission centered at 650 nm in GO aqueous dispersion, for which the intensity is affected by pH and ionic strength. Oxygen-plasma-treated graphene also showed a broad-band fluorescence in the red and NIR region centered at 650 nm. Chhowalla and co-workers,²³ however, found that GO films and aqueous dispersion emit blue fluorescence (325–500 nm with a peak maximum around 390 nm for film and 440 nm for the dispersion). Subrahmanyam, Rao, and co-workers also found that graphene oxidized by H_2SO_4 – HNO_3 emits blue fluorescence.²⁴ On the basis of these reports, there are two types of emission bands for GO: the first is a sharp blue band around 440 nm, the second is a long wavelength (LW) broad band with maximum around 650 nm. The two bands, however, have been studied and reported separately. It is not clear whether and how the two bands are related each other. The inconsistency on the band position of GO emission in the literature shows that GO fluorescence is different from the typical aromatic organic molecules, and more detailed investigations are needed to elucidate the mechanism. In particular, the fluorescence lifetime, which is the important parameter for optoelectronic applications and fluorescence mechanism study, has never been reported. Fluorescence lifetime values are also essential for the

Received: February 22, 2012

Revised: May 7, 2012

Published: June 12, 2012

application of GO in fluorescence lifetime imaging microscopy (FLIM),²⁵ a new fluorescence microscopy technology. Fluorescence lifetime imaging makes it possible to obtain information on the molecules while observing a living cell. The factors that affect the fluorescence lifetime of GO, such as metal or hydrogen ion intensity, hydrophobic properties, oxygen concentration, and molecular binding in cellular tissues, can be measured by FLIM. FLIM allows one to perform more accurate ion concentration measurement over conventional fluorescence microscopy since lifetime is independent of dye concentration, photobleaching, light scattering, and excitation light intensity.²⁵

On the basis of these considerations, we wish to report hereby the fluorescence lifetime of GO under various conditions, the mutual correlation, and transformation of the blue and the LW band. The different emission mechanisms for the two bands are also discussed based on the results. The substituents on GO sheets provide good hydrophilicity and large interlayer steric hindrance for aggregation, both of which facilitate GO to be much easier dispersion as single layered sheets in aqueous solution, and make fluorescence measurement in the aqueous phase possible. The limited solubility of GO in most organic solvents limits our photophysical study on solvent effect.

EXPERIMENTAL SECTION

The synthesis and characterization of GO and chemically derived graphene (CDG) were already described by us previously.²⁶ Deionized water was further purified by Millipore Milli-Q system. All other materials were analytical grade and commercially available.

UV–vis absorption measurements were made with a Hitachi U-4100 spectrophotometer in 10 mm quartz cuvettes. Fluorescence spectra and lifetimes were monitored using Edinburgh Instruments FLS 920 in 10 mm quartz cuvettes, and a filter that cuts off the excitation light but allows emission pass was used before focusing and collecting fluorescence on the emission arm.

All measurements were carried out at room temperature of 22 °C. All fluorescence spectra were corrected for the sensitivity of the photomultiplier tube. All solutions were air saturated. The largest pH used was 9.2, which corresponds to $[\text{OH}^-] = 1.59 \times 10^{-5}$ mol/L. This is much lower than that (1 mol/L NaOH) needed for reducing GO.

RESULTS AND DISCUSSION

Dual Emission of GO. The preparation and characterization of GO and rGO have been described previously.²⁶ GO aqueous dispersion is acidic due to the deprotonation of its COOH groups and –OH groups. The pH value was measured to be 4.7 for our GO dispersion (0.2 mg/mL) in ultra pure water; the acidity is mainly contributed by –COOH groups rather than –OH substituents, since the pH value of 4.7 is closer to the pK_a of –COOH on aromatic rings (ca. 4.2) rather than that of –OH (ca. 9). The fluorescence property of an aromatic acid is very different from its conjugated base because of the change of fluorophores upon deprotonation, similar to the case of fluorescein or rhodamine and their derivatives.^{27–31} It is therefore necessary to control pH for the measurement of GO fluorescence.

We measured the fluorescence spectra and emission decay kinetics under five different pH values (2.5, 5.0, 6.9, 8.3, and

9.2) by dispersing GO solid in buffer solutions under the same ionic strength of 0.01.

The LW band and the blue band of GO have been observed separately by different authors. However, it is still not clear whether the two bands are related and originated from the same excited state.

In fact, two bands can be coexistent and recorded by controlling experimental parameters carefully. By exciting at 300 nm in pH 2.5 buffer, at which the absorbance was controlled at 0.10 (so that the sample is sufficiently low concentrated), GO showed broad band fluorescence all the way from 320 to 1300 nm (Figure 1), which consists of two main

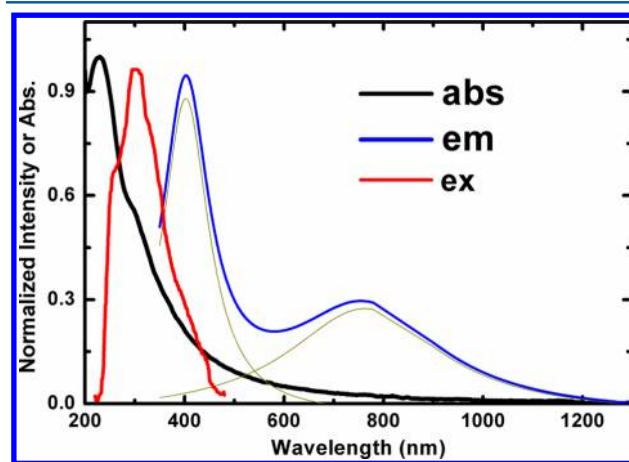


Figure 1. Normalized absorption, fluorescence emission, and fluorescence excitation spectra of GO (0.048 mg/mL) in aq. dispersion at pH 2.5. Excitation wavelength for emission spectrum: 300 nm. Emission wavelength for excitation spectrum: 520 nm.

bands with maximums at 400 (blue band) and 740 nm (LW band), respectively. While the blue band is relatively sharp, the LW band is much broader, covering 350–1250 nm. The peak position and intensity of either band, however, are strongly affected by GO concentration $[\text{GO}]$, pH, and excitation wavelength (λ_{ex}), as discussed below.

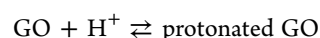
The maximum absorption occurred at 230 nm with a shoulder at 300 nm, which is usually assigned to the $n-\pi^*$ transition of the $\text{C}=\text{O}$ in GO.³² In contrast to its emission, GO absorption spectrum is not sensitive to its concentration and pH.

The shape of the emission spectrum is strongly affected by $[\text{GO}]$. With the increase of $[\text{GO}]$, the emission maximum is gradually red-shifted, and the bandwidth became broader. The blue emission shows up only when $[\text{GO}]$ is sufficiently low due to self-absorption (i.e., the inner filter effect) to its fluorescence.³³ The distortion of its band shape can occur as a result of reabsorption of emitted radiation when $[\text{GO}]$ is moderately high. This effect is much stronger in the UV and blue region than the red and NIR range since GO absorption in the UV and blue region is much more intense (Figure 1 absorption spectrum). When the absorbance A_λ at an emission wavelength is larger than 1, more than 90% of the blue emission is reabsorbed (since $I_a/I_0 = 1 - 10^{-A}$, when $A \geq 1$, $I_a/I_0 \geq 1 - 10^{-1} = 0.90$, in which I_a and I_0 are the absorbed and incident light intensity, respectively), so that little blue emission remained. This partially explains why some studies observed only the LW band; the other reason is that the excitation was

selected at 450 nm or larger, longer than the blue emission maximum.

Also important is the use of filter glass to remove not only Raman and Raleigh scattering but also the diffraction and refraction of GO sheets to the excitation beam (the latter is usually absent for small organic fluorophores). Without the filter glass, the spectra recorded were significantly noisy.

Transformation between the Blue Band and the LW Band. As shown in Figure 2, the relative intensity of the blue emission over the red one is also determined by pH and λ_{ex} . High pH values favor the blue emission (Figure 2 top), while low pH values increase the importance of LW band. The decrease of LW band is accompanied by the increase of the blue band. An isosbestic point occurred at ca. 530 nm, indicating the GO protonation equilibrium:



The LW band turned out to be much less important when pH is close to 7 or greater (Figure 2 top). The LW band is higher than the blue band in pH 2.5 buffer but becomes lower when pH is greater than 5. The LW band is particularly strong at pH 2.5, indicating that protonated GO is mainly responsible for LW band, while the blue band is associated with GO itself.

For the influence of λ_{ex} on the relative height of the two bands, we take the example in pH 2.5 buffer; the LW band is lower when λ_{ex} is 280, 300, 340 nm, but it becomes higher when λ_{ex} is increased to 360 and 380 nm (Figure 2 middle). In pH 5.0, 6.9, and 8.0 buffers, however, the blue band is always higher than the LW band (Figure 2 bottom) owing to the absence of protonated GO, and the band maximum shows a gradual red shift upon λ_{ex} increase.

The excitation spectrum of GO is also profoundly affected by emission wavelength (λ_{em}) and pH, as shown in Figure 3. The longer the emission wavelength was set, the higher and broader the excitation spectra became, since more emitting species are involved in LW emission. This is true under every pH. The λ_{em} effect on GO excitation spectra is consistent with the proposal that GO contains a number of π -conjugated carbons C_n ($n = 2, 3, 4$,

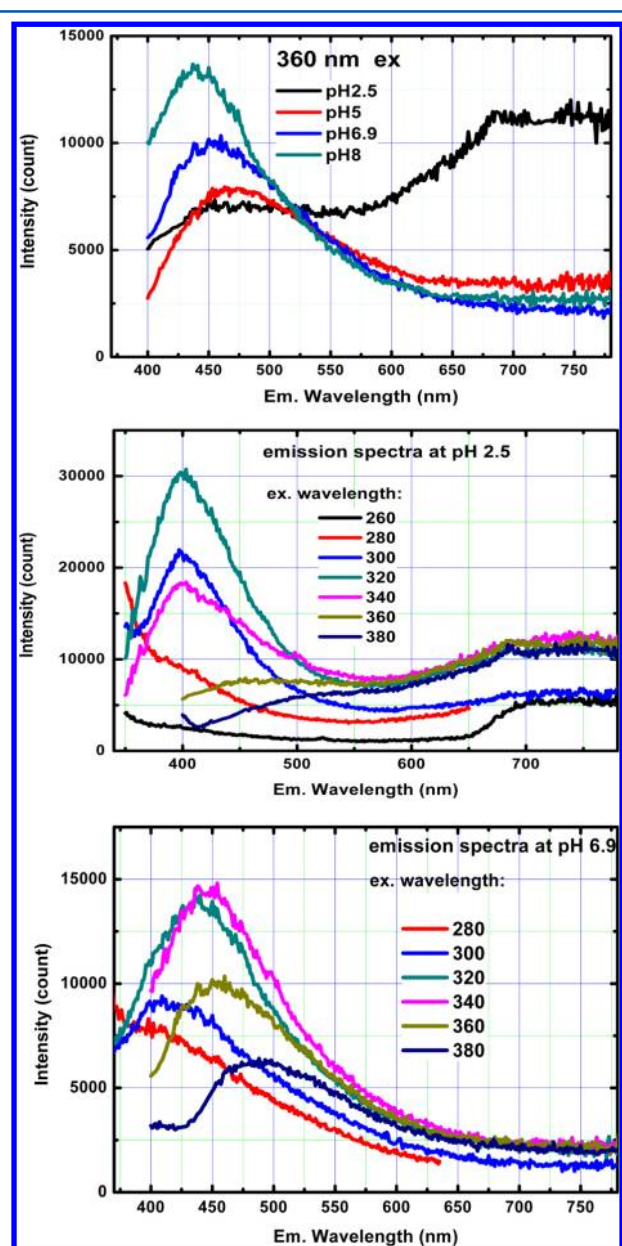


Figure 2. pH and excitation wavelength effect on the relative height of the blue band over the LW band of GO emission. Experimental conditions are included in the figures. The absorption maximum for the sample was adjusted to be 0.10 to avoid inner filter effect.

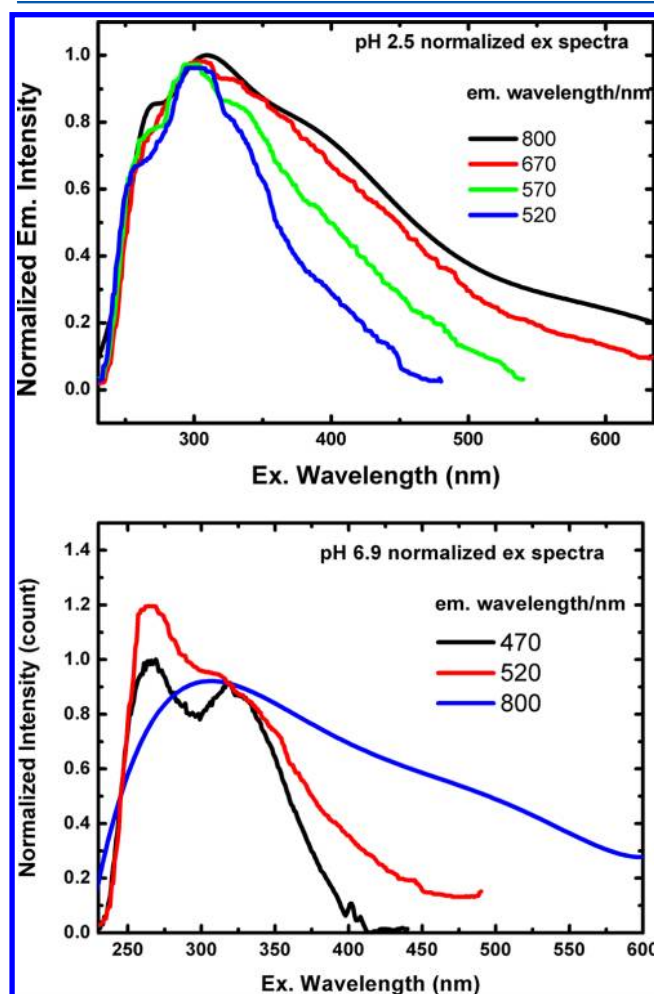


Figure 3. Excitation spectra of GO at pH 2.5 and pH 6.9. Experimental conditions are included inside the figures. The absorption maximum for the sample was adjusted to be 0.10 to avoid inner filter effect.

...).^{5,23,34} The emission and excitation maximum are generally red-shifted upon the increase of n , which explains the observation.

The Nature of the Two Emissions: $n-\pi^*$ or $\pi-\pi^*$ Transitions. Although the fluorescence emission and excitation of GO are strongly affected by pH, its absorption is not the case (Figure 4). A close examination reveals that only

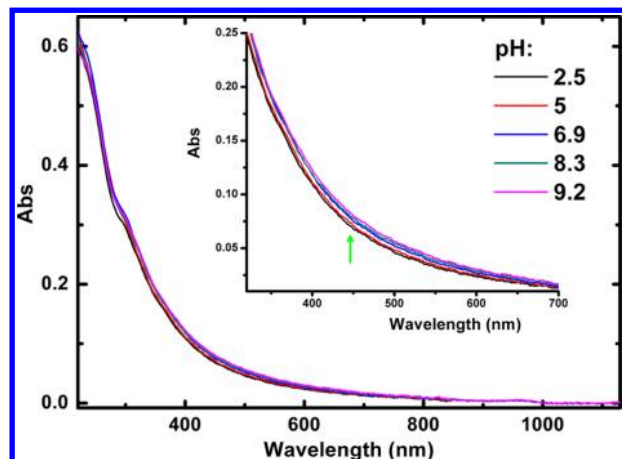


Figure 4. The absorption spectrum of GO (0.032 mg/mL) upon pH change. Inset is the amplified view from 320 to 700 nm.

a very slight increase in absorbance occurred for wavelengths above 310 nm upon pH change (Figure 4). The excitation spectrum contains no 230 nm band (Figure 3), which is the main peak of GO absorption, as shown in Figure 1, suggesting that this main band gap absorption makes no contribution to GO fluorescence, i.e., the emission is not correlated to the band gap electronic transition in GO semiconductor. The excitation does contain the band at ca. 320 nm of the $n-\pi^*$ transition (Figures 3 and 1), indicating that part of the emission is from the $n-\pi^*$ transition. The LW band, on the other hand, has been attributed to aromatic carbon clusters, i.e., transition of $\pi-\pi^*$ type.^{5,23,34} The sp^2 carbon clusters are also present in amorphous carbon and cause fluorescence centered at 700 nm, also due to the transition of $\pi-\pi^*$ type.³⁵

Comparing the excitation at different pH values (Figure 3), one could see that the 320 band due to $n-\pi^*$ transition is blue-shifted to 300 nm when pH is varied from 6.9 to 2.5. This blue shift is obviously due to the protonation of $C=O$ forming $C=OH^+$, which corresponds to the remarkable enhancement of emission intensity. This is consistent with the fact that neutral fluorophores containing $C=O$ are generally non- or weakly fluorescent (since the highest occupied molecular orbital to lowest unoccupied molecular orbital (HOMO–LUMO) electronic transition is of $n-\pi^*$ type) but become much higher fluorescent after protonation (since protonation removes the lone electron pair on oxygen and HOMO–LUMO electronic transition becomes $\pi-\pi^*$ type), such as the quinone form of fluorescein and its derivatives.^{28,30,36}

Fluorescence properties are affected by both the ground state and excited state properties of a fluorophore, while absorption changes are merely the reflection of ground state variation. Upon pH variation, GO absorption changes very little, but its fluorescence changes remarkably. This means that (1) the pH effect on GO fluorescence is due to the excited state protonation or deprotonation, because pK_a is generally much larger in an excited state which makes deprotonation much easier, (2) a significant portion of fluorophores is substituted with $-OH$, $-COOH$, or $-C=O$, which are sensitive to pH.

The Nature of the Two Emission Bands Revealed by Fluorescence Lifetime Study. Figure 5a shows the fluorescence decay at 470 nm (blue band) for GO in different pH buffers. GO concentration was kept constant at 0.01 mg/mL; GO sheets are considered to be single-layered under this concentration. All decay curves are apparently non-mono-exponential, indicating the coexistence of multiple emitting species. With the increase of pH, the kinetic curves move upward (Figure 5a). Higher pH favors the deprotonation of GO, therefore the base form of GO shows longer fluorescence lifetime and higher emission efficiency; the latter is consistent with the results in Figure 2 in which the blue band is enhanced by higher pH (Figure 2, top). This pH effect on the blue emission of GO is similar to the case of fluorescein, a dibasic organic acid (H_2F), which also contains $-COOH$, $-OH$, and $-C=O$. For H_2F , its base form F^{2-} shows longer emission

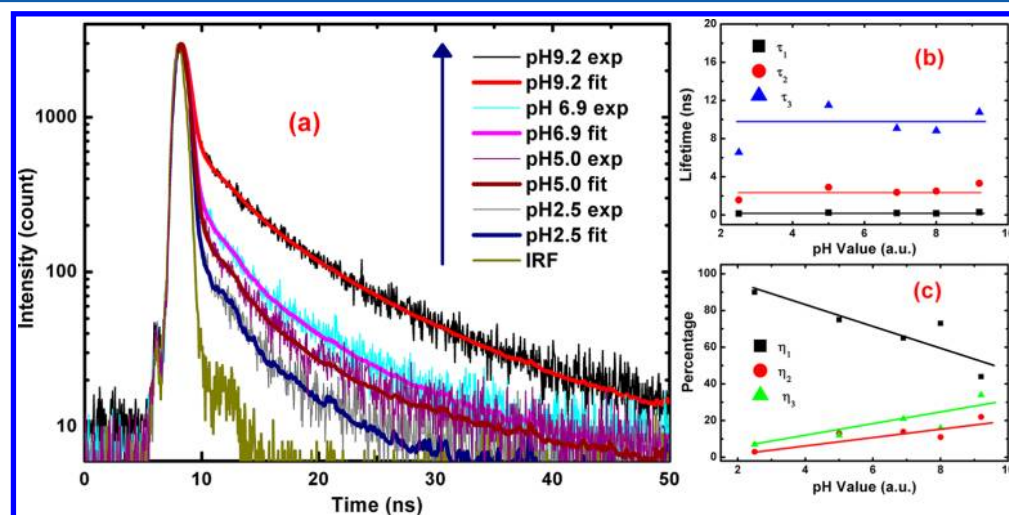


Figure 5. (a) The fluorescence decay at 470 nm for GO in different pH buffers. [GO] was kept constant at 0.024 mg/mL. The excitation wavelength is 379 nm (50 ps diode laser). IRF: instrumental response function. (b) The dependence of the fluorescence lifetime of three fitting components (τ_i , $i = 1, 2, 3$) on pH. (c) The dependence of η_i (percentage contribution to total emission, $i = 1, 2, 3$) on pH.

lifetime (4.1 ns) and higher fluorescence quantum yield (0.92) than that of HF^- (3.0 ns, 0.35), while the H_2F^+ excited state is too short-lived to be fluorescent.³⁰

Although more than three emitting components are expected in GO, all the decay traces can be fit by triple exponential functions mathematically. The lifetimes are 0.20 ± 0.05 (τ_1), 2.5 ± 0.8 (τ_2), and 9.2 ± 2.5 (τ_3) ns, respectively; while χ^2 values are within 1.30 ± 0.12 .

The lifetime τ_i ($i = 1, 2, 3$) is not very sensitive to pH (Figure 5b) in contrast to η_i (the percentage contribution of an emitting component i to total emission). η_i is strongly determined by pH, as displayed in Figure 5c. The shortest-lived emitting components predominate at low pH, but their importance is decreased with the increase of pH; η_2 and η_3 show the opposite trend, as η_3 for the longest lived can reach 35% at pH 9.2. According to the tendency, the long-lived components (τ_2 and τ_3) are mainly due to deprotonated GO and neutral GO (τ_2 and τ_3 are associated with π - π^* emission); the short-lived component (τ_1) in the blue emission (τ_1 is associated with n - π^* emission) is mainly owing to protonated GO. Since the τ_1 value reaches the detection limit of the system, all the contribution from emitting species with shorter lifetime than τ_1 will be included in the component.

τ_3 (close to 10 ns) is significantly longer than that of the autofluorescence of tissues and that of the most often used probes, such as rhodamines and fluoresceins (which are typically shorter than 5 ns). This long lifetime is advantageous in biomedical applications since high signal-to-noise images can be obtained compared to that of the fluorescent dyes normally used.

The fluorescence decay at 680 nm (for the LW band), however, is not significantly dependent on pH as shown at the bottom of Figure 6, indicating that the related fluorophores

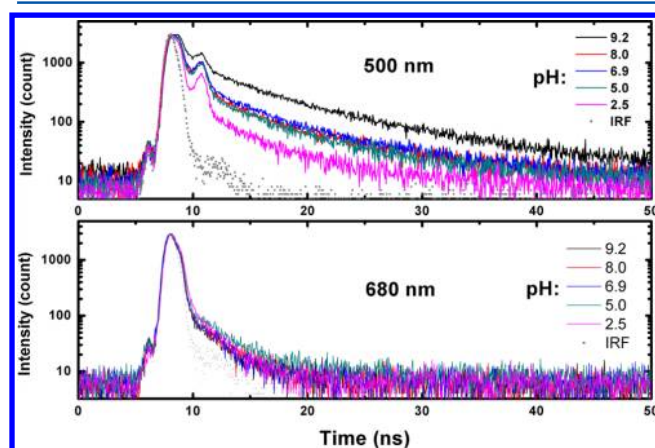


Figure 6. The fluorescence decay at 500 nm (top) and 680 nm (bottom) for GO in different pH buffers. [GO] was kept constant at 0.024 mg/mL. The excitation wavelength is 379 nm of a 50 ps diode laser. IRF: instrumental response function.

contain much less conjugated $-\text{C}=\text{O}$, $-\text{COOH}$, and $-\text{OH}$ groups. LW band decay at 680 nm can be fit by biexponential functions, and the lifetime is $\tau_1 = 0.21 \pm 0.05$ and $\tau_2 = 2.4 \pm 0.5$ ns, respectively. The short-lived component predominates ($\eta_1 = 0.93 \pm 0.03$ and $\eta_2 = 0.07 \pm 0.03$). η_1 and η_2 are little affected by pH. These fluorophores are therefore mainly located in the interior of GO sheets, and the emissive mechanism is due to π - π^* transition, in contrast to the blue band caused by n - π^* transition. The fluorophores associated with n - π^* transition

are expected to locate at the edge of GO sheets, such that $-\text{C}=\text{O}$ can be geometrically fit to the flat π -system of a fluorophore.

The fluorescence of n - π^* transition is generally longer lived due to its low transition probability, and hence smaller fluorescence decay rate constant.

The emission kinetics at the wavelength around 500 nm shows some particularly interesting behavior (Figure 6 top). After the normal decay up to 9.6 ns, an emission rise occurred, it reached maximum at 10.7 ns, and then decayed and finished at 12 ns, suggesting that a new emitting species was formed during the process. The emission lifetime of the new emitting species is about 0.53 ns at pH 2.5. The increase of pH decreased the intensity and slowed the decay kinetics for the new species (top of Figure 6). This phenomenon also occurred at other wavelengths as displayed in Figure 7. The signal is the

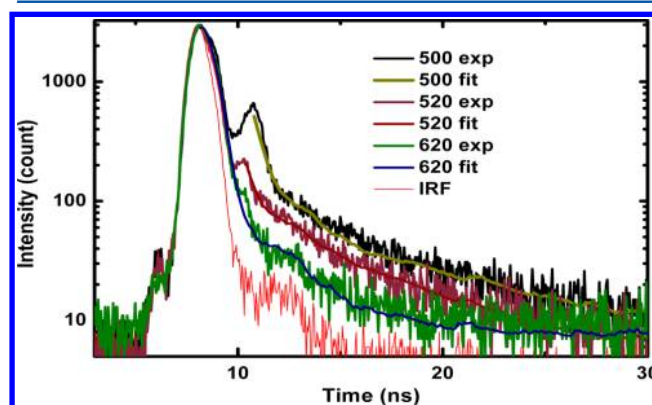


Figure 7. The fluorescence decay at 500, 520, and 620 nm for GO in pH 2.50 buffer. [GO] was kept constant at 0.024 mg/mL. The excitation wavelength is 379 nm of a 50 ps diode laser. IRF: instrumental response function.

strongest at 500 nm, but it became less and less weak with the increase of wavelength. This fact provides evidence that some type of reactions take place from the excited state S_1 , forming an emitting species with the maximum emission at 500 nm and a lifetime of 0.53 ns.

On the pH effect, the decays at pH 2.5 and pH 9.2 are significantly different from each other, and they are also distinguished from the decays at other pHs: 5.0, 6.9, and 8.2. On the other hand, the decays at pH 5.0, pH 6.9, and pH 8.2 are similar (for example, Figure 6, top), as are the pH effects on the steady state fluorescence spectra of GO. This is apparently because the affected fluorophores are likely fully protonated at pH 2.5, completely deprotonated at pH 9.2, and in mixed forms at other pH values.

The kinetic decay of GO is also dependent on emission wavelength, as shown in Figure 3.

Combining the results of steady state and time-resolved studies, it is clear that the emission lifetime, emission spectrum, and excitation spectrum are wavelength dependent. This shows that GO fluorescence is different from any single organic emitting species containing π -system, for which the emission lifetime and spectral properties are independent of wavelength. GO, even if in single-layered sheets, consists of a large number of independent chromophore (fluorophore) of different sizes connected by covalent C-C bonds. Each chromophore is an aromatic sub- π -system formed by sp^2 -hybridized carbon atoms, while each subsystem may be of different sizes and is

surrounded by sp^3 carbon atoms. The strong pH and wavelength effect also suggests that the emission is not due to band-edge transitions as is the case in typical semiconductors, but is rather similar to the case of aromatic organic molecules, i.e., the fluorescence in GO arises from $S_1 \rightarrow S_0$ transitions. GO samples prepared by different methods under varied conditions may contain a set of different sp^2 clusters. GO emission is also affected by excitation wavelength. It is therefore understandable that discrepancies exist in the emission of GO solid films,^{23,24} even in the absence of pH changes.

CONCLUSIONS

To reveal the nature of the dual emission of GO, we have measured the fluorescence lifetime, fluorescence emission, and excitation spectra, as well as UV-vis and NIR absorption spectra under various conditions, including excitation (or emission) wavelength, pH, and GO concentration. For the first time, we showed that the blue band (ca. 440 nm) and LW band (ca. 700 nm) can be recorded simultaneously by carefully selecting the concentration, excitation wavelength, and pH values. The blue band is favored by low GO concentration, short excitation wavelength, and high pH value, while the LW band is favored by low pH and long excitation wavelength. Two bands are closely related by the protonation or deprotonation of GO. The blue band contains three emitting components; one of them has a lifetime as long as 10 ns, and its emitting intensity is fairly sensitive to pH, showing the potential for applications in sensing H^+ and fluorescence lifetime imaging. Combining the results under various conditions, we conclude that the electronic transition for this component is very likely due to $n-\pi^*$ transition. The LW band contains two main emitting components (0.2 and 2.1 ns) that also appear in the blue band as minor contributors; the related emission is assigned to $\pi-\pi^*$ transition. Due to the broadband emissive (300–1250 nm), long-lived, pH sensitive, and excitation wavelength-dependent properties, GO emission can be tailored easily for versatile applications.

AUTHOR INFORMATION

Corresponding Author

*E-mail: zhangxianfu@tsinghua.org.cn.

Notes

The authors declare no competing financial interest.

ACKNOWLEDGMENTS

This work has been supported by the Hebei Provincial Science Foundation (Contract B2010001518) and HBUST.

REFERENCES

- (1) Huang, X.; Qi, X.; Boey, F.; Zhang, H. *Chem. Soc. Rev.* **2012**, *41*, 666.
- (2) Zhu, Y.; Murali, S.; Cai, W.; Li, X.; Suk, J. W.; Potts, J. R.; Ruoff, R. S. *Adv. Mater.* **2010**, *22*, 3906.
- (3) Loh, K. P.; Bao, Q.; Eda, G.; Chhowalla, M. *Nat. Chem.* **2010**, *2*, 1015.
- (4) Bonaccorso, F.; Sun, Z.; Hasan, T.; Ferrari, A. C. *Nat. Photonics* **2010**, *4*, 611.
- (5) Sun, X.; Liu, Z.; Welsher, K.; Robinson, J. T.; Goodwin, A.; Zaric, S.; Dai, H. *Nano Res.* **2008**, *1*, 203.
- (6) Loh, K. P.; Bao, Q.; Ang, P. K.; Yang, J. *J. Mater. Chem.* **2010**, *20*, 2277.
- (7) Chen, D.; Tang, L.; Li, J. *Chem. Soc. Rev.* **2010**, *39*, 3157.
- (8) Allen, M. J.; Tung, V. C.; Kaner, R. B. *Chem. Rev.* **2010**, *110*, 132.
- (9) Rao, C. N. R.; Sood, A. K.; Subrahmanyam, K. S.; Govindaraj, A. *Angew. Chem., Int. Ed.* **2009**, *48*, 7752.
- (10) Geim, A. K. *Science* **2009**, *324*, 1530.
- (11) Geim, A. K.; Novoselov, K. S. *Nat. Mater.* **2007**, *6*, 183.
- (12) Huang, X.; Yin, Z.; Wu, S.; Qi, X.; He, Q.; Zhang, Q.; Yan, Q.; Boey, F.; Zhang, H. *Small* **2011**, *7*, 1876.
- (13) He, Q.; Wu, S.; Yin, Z.; Zhang, H. *Chem. Sci.* **2012**, DOI: 10.1039/C2SC20205K.
- (14) He, Q. Y.; Sudibya, H. G.; Yin, Z. Y.; Wu, S. X.; Li, H.; Boey, F.; Huang, W.; Chen, P.; Zhang, H. *ACS Nano* **2010**, *4*, 3201.
- (15) Cao, X. H.; He, Q. Y.; Shi, W. H.; Li, B.; Zeng, Z. Y.; Shi, Y. M.; Yan, Q. Y.; Zhang, H. *Small* **2011**, *7*, 1199.
- (16) Yin, Z. Y.; Wu, S. X.; Zhou, X. Z.; Huang, X.; Zhang, Q. C.; Boey, F.; Zhang, H. *Small* **2010**, *6*, 307.
- (17) Yin, Z. Y.; Sun, S.; Salim, T.; Wu, S. X.; Huang, X.; He, Q. Y.; Lam, Y. M.; Zhang, H. *ACS Nano* **2010**, *4*, 5263.
- (18) Chen, J. L.; Yan, X. P. *Chem. Commun.* **2011**, *47*, 3135.
- (19) Cuong, T. V.; Pham, V. H.; Tran, Q. T.; Hahn, S. H.; Chung, J. S.; Shin, E. W.; Kim, E. J. *Mater. Lett.* **2010**, *64*, 399.
- (20) Chen, J. L.; Yan, X. P. *J. Mater. Chem.* **2010**, *20*, 4328.
- (21) Luo, Z.; Vora, P. M.; Mele, E. J.; Johnson, A. T. C.; Kikkawa, J. M. *Appl. Phys. Lett.* **2009**, *94*, 111909.
- (22) Liu, Z.; Robinson, J. T.; Sun, X.; Dai, H. *J. Am. Chem. Soc.* **2008**, *130*, 10876.
- (23) Eda, G.; Lin, Y. Y.; Mattevi, C.; Yamaguchi, H.; Chen, H. A.; Chen, I.; Chen, C. W.; Chhowalla, M. *Adv. Mater.* **2009**, *22*, 505.
- (24) Subrahmanyam, K. S.; Kumar, P.; Nag, A.; Rao, C. N. R. *Solid State Commun.* **2010**, *150*, 1774.
- (25) Bastiaens, P. I. H.; Squire, A. *Trends Cell Biol.* **1999**, *9*, 48.
- (26) Zhang, X. F.; Xi, Q. *Carbon* **2011**, *49*, 3842.
- (27) Zhang, X. F.; Liu, Q.; Son, A.; Zhang, Q.; Zhao, F.; Zhang, F. *J. Fluoresc.* **2008**, *18*, 1051.
- (28) Zhang, X. F.; Liu, Q.; Wang, H.; Zhang, F.; Zhao, F. *Photochem. Photobiol. Sci.* **2008**, *7*, 1079.
- (29) Martin, M.; Lindqvist, L. *J. Luminesc.* **1975**, *10*, 381.
- (30) Sjöback, R.; Nygren, J.; Kubista, M. *Spectrochim. Acta, Part A* **1995**, *51*, L7.
- (31) Mchedlov-Petrosyan, N. O.; Vodolazkaya, N. A.; Gurina, Y. A.; Sun, W.-C.; Gee, K. R. *J. Phys. Chem. B* **2010**, *114*, 4551.
- (32) Luo, Z.; Lu, Y.; Somers, L. A.; Johnson, A. T. C. *J. Am. Chem. Soc.* **2009**, *131*, 898.
- (33) Kubista, M.; Sjöback, R.; Eriksson, S.; Albinsson, B. *Analyst* **1994**, *119*, 417.
- (34) Luo, Z.; Vora, P. M.; Mele, E. J.; Johnson, A. T. C.; Kikkawa, J. M. *Appl. Phys. Lett.* **2009**, *94*, 111909.
- (35) Henley, S. J.; Carey, J. D.; Silva, S. R. P. *Appl. Phys. Lett.* **2004**, *85*, 6236.
- (36) Zhang, X.; Liu, Q.; Son, A.; Zhang, Q.; Zhang, F.; Zhao, F. *Photochem. Photobiol. Sci.* **2008**, *7*, 299.